Brodogradnja Volume 77 Number 4 (2026) 77403

journal homepage: www.brodogradnja.fsb.hr

Brodogradnja

An International Journal of Naval Architecture and Ocean Engineering for Research and Development

Experimental study on piling and penetration behavior of jack-up offshore platforms on layered seabed foundations

Zailiang Liu[1,3], *Jin Shi*[2], *Xiaobin Li*[1], *Yonghe Xie*[2], *Zhi Xu*[2], *Chenyang Liu*[2], *Yuelin Song*[2,*]

[1]*School of Naval Architecture, Ocean and Energy Power Engineering, Wuhan University of Technology, Wuhan 430063, China*
[2]*School of Naval Architecture and Maritime, Zhejiang Ocean University, Zhoushan 316022, China*
[3]*School of Marine Equipment Engineering, Zhejiang International Maritime College, Zhoushan 316021, China*

ARTICLE INFO

Keywords:
Jack-up platform
Piling
Leg penetration
Experimental system
Hydraulic control

ABSTRACT

This study aims to design a novel experimental system for replicating the bearing capacity behavior of layered seabed foundations during the process of leg piling and penetration. A test apparatus for a jack-up offshore platform was developed, with a telescopic pile foundation hydraulic cylinder mounted at the base of platform leg to achieve experimental investigation of penetration behavior through layered seabed soils. A servo-hydraulic system model was developed by incorporating the Proportional-Integral-Derivative (PID) control algorithm into the proportional valve control system, thereby realizing dynamic simulation of various penetration depths and soil bearing capacities through precise hydraulic cylinder pressure regulation. A series of simulation analyses and experimental tests were conducted to delve into the variation in bearing capacity during the piling process, with a focus on the influence of soil shear strength, layer thickness, and backfill characteristics. The findings indicate that the experimental system exhibits a high level of accuracy in simulating the bearing capacity of complex layered seabed foundations, with an overall error maintained within 15 %. This study provides an experimental methodology and technical approach for simulating the process of pile leg penetration in the investigation targeting the structural integrity and stability of offshore platforms.

1. Introduction

The jack-up platform serves as a crucial infrastructure for offshore oil-related development. The risk of punch-through failure remains challenging for jack-up platforms during the operation process of pile installation. Prior to the positioning operations, jack-up offshore platforms ensure sufficient and stable support by embedding their legs into the seabed. Upon the completion of operations, these legs are retracted from the seabed, allowing the platform to be relocated to subsequent operational sites. However, the complex and variable geological conditions on the seabed, particularly when jack-up platforms encounter hard-over-soft soil formations, may trigger a sudden penetration of the legs through the hard soil layer - a phenomenon called leg punch-through [1]. Punch-through incidents commonly result in leg damage, platform tilting, or even capsizing, posing substantial risks to the safety of offshore structures. According to statistical evidence, problems associated with seabed foundation account for approximately one-third of jack-up platform

* Corresponding author.
E-mail address: songyl_wut@163.com

https://doi.org/10.21278/brod77403
Received 22 July 2025; Received in revised form 10 March 2026; Accepted 21 March 2026
Available online 8 April 2026
ISSN 0007-215X; eISSN 1845-5859

accidents, with 95 % of global punch-through incidents occurring in alternating hard-soft soil layers [2]. Consequently, leg punch-through has become a research hotspot in industrial and academic fields.

Although the punch-through risk has been addressed in various studies, the dynamical evaluation of layered seabed behavior through hydraulic-controlled simulation platforms has rarely been investigated, leading to a critical gap in validating soil-structure interaction under simulated stratification using real-time loading control systems. To ensure operational safety of jack-up platforms at sea, researchers have extensively studied the foundation bearing behavior during the process of platform leg penetration into seabed soils. The latest advances in finite element modeling have clarified the effects of soil layering and strain hardening on penetration resistance and lateral confinement, thereby enhancing the predictive capability of punch-through scenarios [3]. Martin [4] investigated the settlement behavior of independent leg jack-up drilling platforms, highlighting the significance of leg penetration depth for platform stability. Hossain and Randolph [5] established a penetration resistance model for spudcan foundations in clay through theoretical analysis, revealing the influence of foundation geometry and soil strength on bearing capacity characteristics. Korzani et al. [6] proposed a model based on nonlinear Winkler foundation beam theory for analyzing the insertion process of platform legs into the seabed. Fan et al. [7] simulated continuous penetration of jack-up foundations in various soil profiles using a novel discrete element method. Kong et al. [8] enhanced the prediction accuracy of peak-penetration resistance of spudcan foundations in sand-over-clay and three-layer clay deposits by developing an advanced parameter estimation technique.

Extensive discussion has been made on the factors affecting the bearing capacity of the foundation. Xu et al. [9] proposed a piling calculation method for jack-up drilling platforms, comprehensively considering stratigraphy, spudcan bearing capacity, and pile group effects in the analysis of penetration risk during the piling process. Michalowski and Shi [10] found a positive correlation between the bearing capacity of platform legs and the strength of the underlying clay layer. Randolph et al. [11] and Hosain et al. [12] examined the mechanism through which load magnitude, leg length, and preload ratio affect bearing capacity and load-displacement behavior. Zhang and Liu [13] found that the increase in the embedment ratio and diameter can significantly improve the dynamic stiffness of single pile foundations and disrupt their lateral displacement. Yi et al. [14] investigated post-installation consolidation settlement of leg foundations on clay seabeds through numerical simulations, highlighting how long-term consolidation affects platform stability. Using both centrifuge tests and numerical simulations, Zhang et al. [15] integrally studied the vertical bearing capacity of jack-up platform mat foundations in marine clay, so as to clarify the impact of various seabed sediment layers on foundation settlement. To mitigate punch-through risk during the process of platform piling, Zhao et al. [16] assessed penetration risk by calculating the complete resistance profile of dense sand underlying clay layers. Kellezi et al. [17] urged upon the importance of accurate geotechnical investigations, soil parameter assessments, appropriate modeling strategies, and controlled load increment procedures in improving analysis accuracy. Houlsby et al. [18] and Osborne et al. [19] recommended the application of active punch-through or gap reduction methods for preloading single piles, while emphasizing the necessity of strict control regarding penetration depth.

The complexity and variability of seabed stratigraphy, especially in the presence of hard-over-soft soil formations, may sudden penetration of platform legs through the upper hard soil layer, namely, leg punch-through [20], posing substantial risks to the safe operation of jack-up platforms. Conventional seabed soil simulation methods fail to accurately capture the real variability of seabed conditions, especially the spatial heterogeneity of soils beneath individual legs, variations in soil properties under different legs on identical platforms, and progressive soil hardening under increasing load.

This study presents the development of a hydraulic experimental system designed to simulate seabed soils and effectively replicate the displacement-resistance response observed during the piling process of complex layered seabed foundations. Unlike centrifuge testing, physical modeling, and DEM-based numerical simulations reliant on configuring actual soil layers [10, 11, 15], the proposed hydraulic platform simulates layered soil bearing capacity through a hydraulic mechanism to achieve repeatable and real-time control of soil resistance without the need for physical soil reconstruction, which is experimentally efficient, and parametrically flexible. The system dynamically simulated various penetration depths and soil bearing capacities through precise pressure regulation by implementing a combined model of a proportional valve and

hydraulic cylinder through the Proportional-Integral-Derivative (PID)-based control algorithm. Additionally, a punch-through testing method for jack-up offshore platforms was devised, leveraging hydraulic servo closed-loop control to clarify the interaction between platform legs and soil, as well as the response characteristics of seabed layers with varying depths and hardness in punch-through events. A composite test platform integrating hydraulic servo control and platform elevation systems was developed, employing an independently designed hydraulic telescopic mechanism in conjunction with a leg structure to realize high-precision simulation of the dynamic mechanical behavior in multilayer seabed soils with varying depths and stiffness. The present study allows for real-time simulation of potential deep-seabed hazard evolutions and provides reliable technical support for analyzing and preventing punch-through issues during the operational process of platform piling.

This paper is structured as follows: Section 2 describes the experimental system and simulation model; Section 3 presents the experimental procedures and results; Section 4 discusses the effects of various soil parameters; and Section 5 summarizes the key findings and future directions.

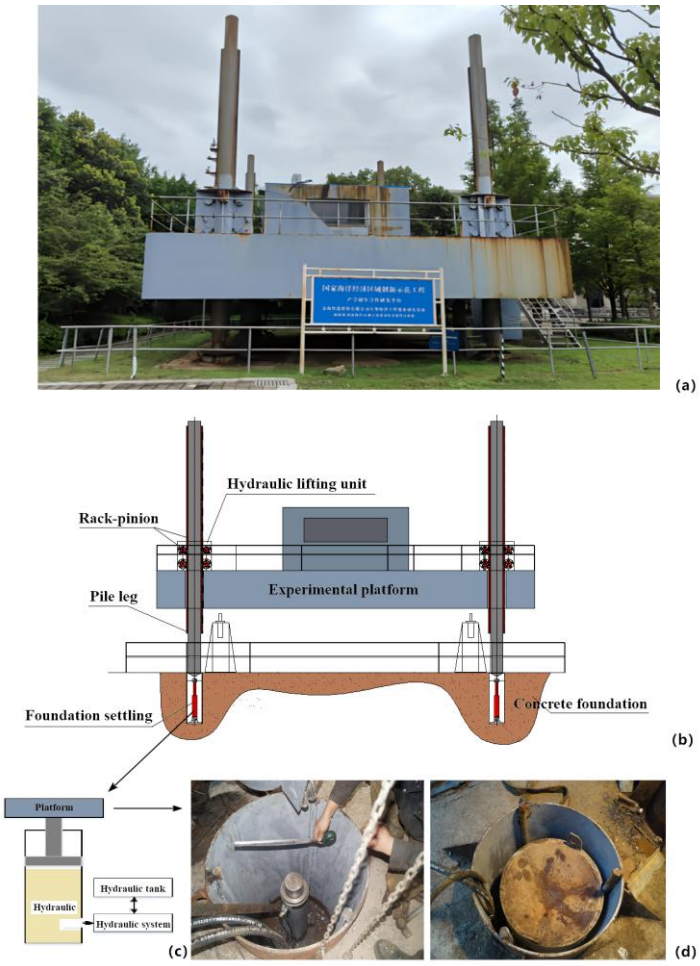

Fig. 1 Jack-up offshore platform piling simulation experiment: (a) experimental site, (b) design schematic, (c) foundation simulation system design, and (d) hydraulic damping mechanism

2. Jack-up offshore platform piling simulation experiment

2.1 Offshore platform piling experimental apparatus

In this study, a large-scale jack-up offshore simulation platform was constructed. The primary structure features a steel rectangular configuration with four legs, measuring 15 m × 10 m × 1.5 m (length × width × height), with a total weight exceeding 30 t, as shown in Figure 1. An integrated control room was positioned at the top of the platform. Each leg base incorporates a hydraulic damping mechanism capable of simulating seabed piling and settlement, facilitating the seamless integration of the platform structure, lifting mechanism, legs, and seabed simulation. This study employed a hydraulic telescopic mechanism in place of physical soil

layering. Multiple geotechnical bearing capacities were simulated by adjusting the input signal of the hydraulic servo-controlled damping system. This system allowed for the simulation of the operational behavior regarding major offshore facilities under hazardous conditions, shedding light on the settlement behavior of platform legs.

2.2 Damped hydraulic system for piling

This study conducted a simulation analysis of the jack-up offshore platform piling damping hydraulic system using the AMESim simulation platform. The servo-hydraulic simulation system comprises four core functional modules: target soil curve generation, scaling transformation, hydraulic control execution and error validation as illustrated in Figure 2.The simulation model primarily consists of the following components: coarse filter, pump-motor unit, fine filter, relief valve, solenoid directional valve, proportional pressure valve, bidirectional hydraulic lock, and hydraulic cylinder, as shown in Figure 3. Through a series of comparative analyses and in combination with the parameters of the market equipment models, the selection of the device was completed, as shown in Appendix A. The simulation process involves four key steps: system modeling, sub-model selection, parameter configuration, and simulation execution. Within the system, predetermined pressure was exerted on a mass block to facilitate the downward motion of the piston. Displacement and pressure sensors were applied for data collection throughout the process. Both hydraulic fluid velocity and flow rate were variable.

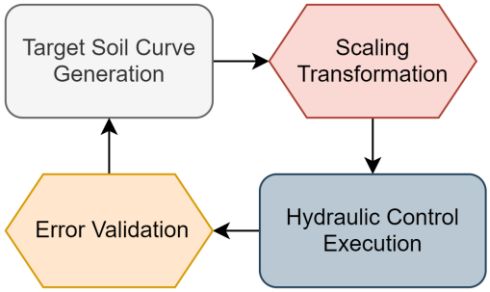

Fig. 2 schematic conceptual diagram

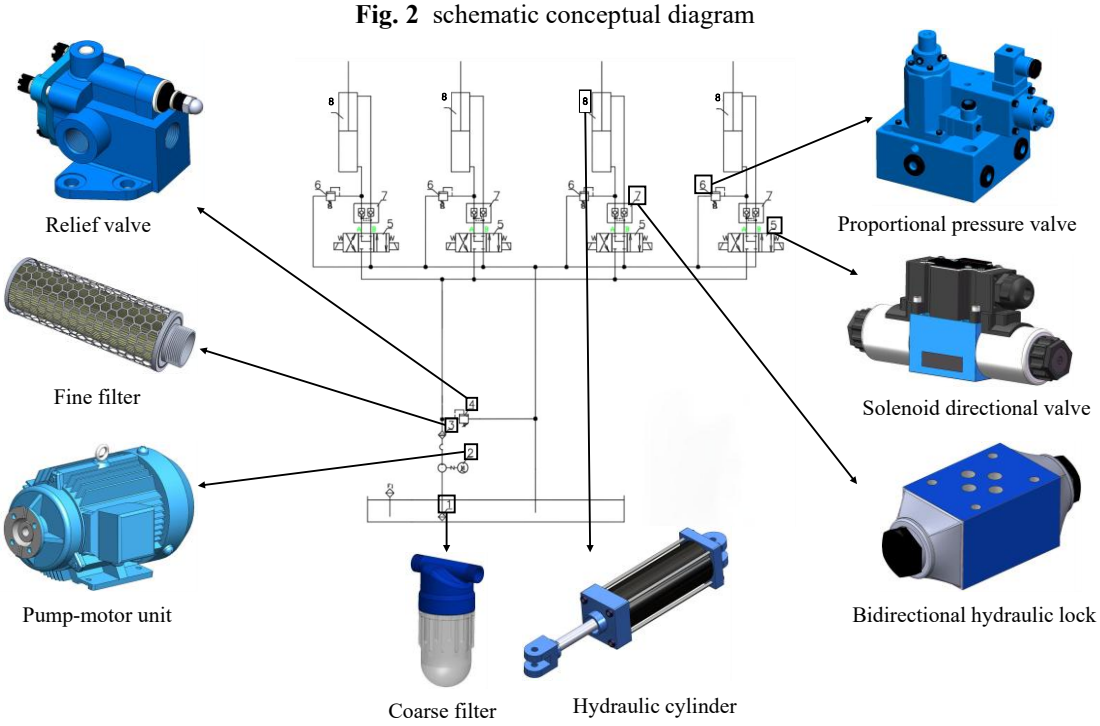

Fig. 3 Hydraulic system simulation model

Upon the activation of the proportional pressure valve, variations in input electrical signal adjusted the opening of the valve to control the flow and pressure of hydraulic oil, ultimately regulating the downward motion of the piston cylinder. In a punch-through event, the energized and de-energized states of the solenoid

valve were altered to reposition the spool valve, which changed the flow direction of the hydraulic fluid and lifted the affected piston cylinder. This process was monitored and analyzed via the data feedback module to assess the overall system behavior. The effect of temperature on the overall system was overlooked during the modeling process.

In the present study, a programmable hydraulic actuator was installed at the bottom of the pile legs of the experimental platform. Consequently, the hydraulic force can be dynamically adjusted in accordance with the pre-defined geological properties, to simulate the resistance variations of soil at different depths, thereby achieving a refined simulation of the pile insertion process. The top and side walls of the hydraulic chamber are fixed, and the bottom boundary is modeled as rigid; foundation deformation under loading is assumed to be negligible. To ensure dynamic similarity between the hydraulic simulation and actual seabed geotechnical behavior, geometric, force, and kinematic similarity criteria are rigorously satisfied. Accounting for scale effects, the hydraulic pressure P is equated to the seabed's unit-area bearing capacity q via the following equivalent relationship:

$$q=P\frac{A_C}{A_S} \tag{1}$$

where, A_C is the piston area of the hydraulic cylinder, and A_S represents the bottom area of the pile leg.

The influence of specific soil properties on pile resistance is explicitly accounted for in the displacement-resistance relationship used in pile driving analysis. The displacement of the pile cap penetration is governed by the following Equation (2), where D_{TR} denotes the displacement, and the bearing capacity of each soil layer is regulated through Equation (3) with the input signal of the proportional valve control system. In simulation and experimental setups, the penetration rate of pile legs depends on the soil profile and testing objectives.

$$\begin{cases} D_R=mD_{TR} \\ D_{TC}=mD_c \end{cases} \tag{2}$$

where D_{TR} denotes the displacement at the insertion point, D_R signifies the displacement regulated by hydraulic control, D_{TC} represents the feedback displacement, D_C stands for the actual displacement, and m represents the conversion ratio coefficient.

$$\begin{aligned} U_R &= \beta \cdot F_{TR} \\ F_{TC} &= \frac{\beta}{14} U_{TC} \end{aligned} \tag{3}$$

where, U_R denotes the input signal voltage, F_{TR} represents the actual bearing capacity, β stands for the conversion coefficient, U_{TC} is the feedback signal voltage, and F_{TC} represents the actual output bearing capacity.

2.3 Hydraulic PID control system

This study achieved control objectives by introducing a PID controller to adjust the operating state of the hydraulic system, as shown in Figure 4. The control algorithm executed closed-loop regulation by evaluating the discrepancy between the predetermined target value of the controlled system and the real-time output signal. The algorithm dynamically adjusted control parameters according to Equation (4), forming an error feedback correction mechanism that continuously reduced the deviation between the actual operating state and the desired state of the system, ensuring error convergence within an acceptable range to meet control objectives.

In the proportional valve-controlled hydraulic system, displacement sensors collected real-time actual output data of the hydraulic system and fed these data back to the PID controller. The PID controller calculated the error between the feedback data and the actual command and output a control signal accordingly. The proportional valve regulated the flow and pressure of the hydraulic system based on the control signal to execute the corresponding hydraulic actions. The controller employs the PORT0 communication interface at

a baud rate of 209.6 kbps to guarantee real-time and dependable data transmission. The sampling frequency is 50 Hz. The 3dB bandwidth of the hydraulic proportional valve is 10 Hz. Through real-time adjustment by the PID controller, the hydraulic system gradually approached and stabilized adjacent to the desired value, achieving precise control of the hydraulic system. The improved overall hydraulic simulation model is shown in Figure 5. Following the implementation of PID closed-loop control, the steady-state and dynamic performance of the system were significantly improved, as shown in Figure 6. Specifically, the output displacement can more accurately track the set value, with reduced overshoot and oscillations. The PID coefficients were empirically tuned based on step response trials to minimize steady-state error and overshoot, ensuring system stability during the process of penetration simulation.

To enable a meaningful comparison between the hydraulic simulation and actual seabed behavior, a proportional mapping framework was adopted, including the conversion factors of stiffness and bearing pressure based on the principles of dimensional similarity and calibration against empirical soil behavior curves. The hydraulic pressure exerted on the telescopic cylinder was assumed to be proportional to equivalent seabed bearing capacity per unit depth.

Upon the reception of the step signal, the system fails to respond instantaneously due to inherent dynamic delays, encompassing hydraulic fluid compressibility, valve spool dead-zone, and mechanical friction, resulting in a transient delay in the response curve. Subsequently, under the combined effect of P and I control actions, the system commences to ascend, and the ascent rate is regulated by the respective P and I parameters. As the system approaches the target value, the D component becomes operative, counterbalancing the high inertia of the hydraulic system. This gives rise to a smooth and gradual convergence towards the set-point, circumventing abrupt overshoot. The implementation of PID control significantly improves the response speed and stability of the system, underpinning the precise control of hydraulic systems.

$$u(k) = k_p e(k) + k_i T \sum_{j=0}^{k} e(j) + k_d \frac{e(k) - e(k-1)}{T} \tag{4}$$

where, k is the sampling index, k_p signifies the proportional gain, and T denotes the sampling interval.

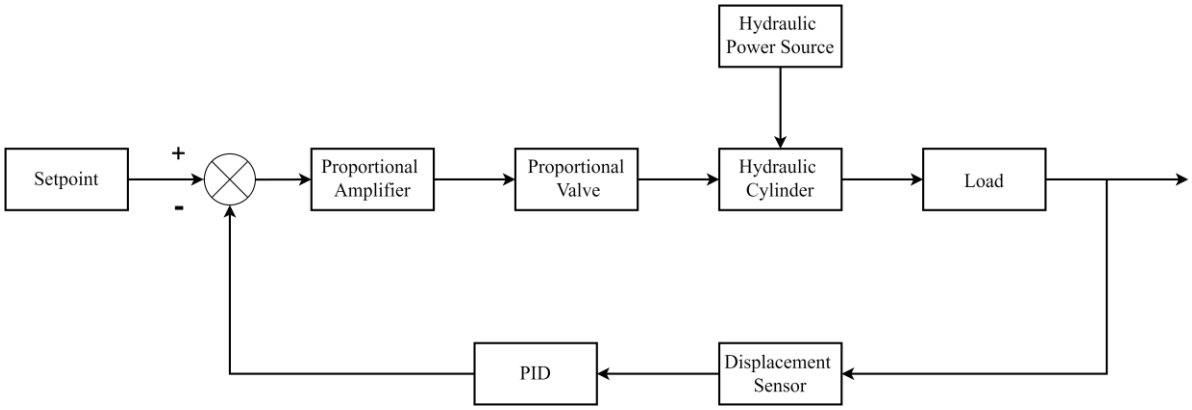

Fig. 4 Schematic diagram of the PID control system

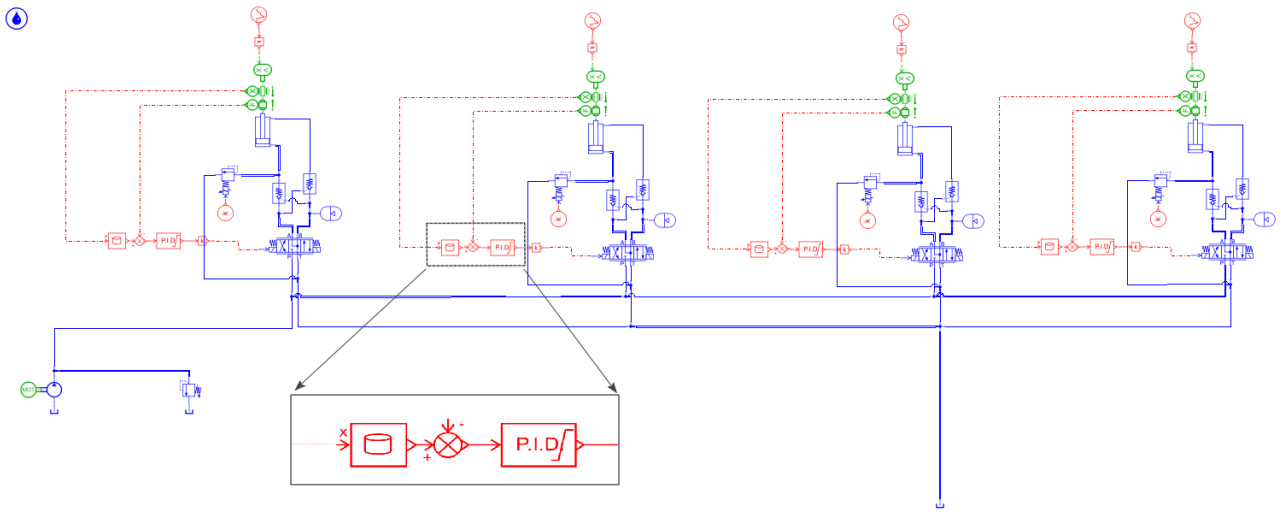

Fig. 5 Simulation model of the hydraulic PID system

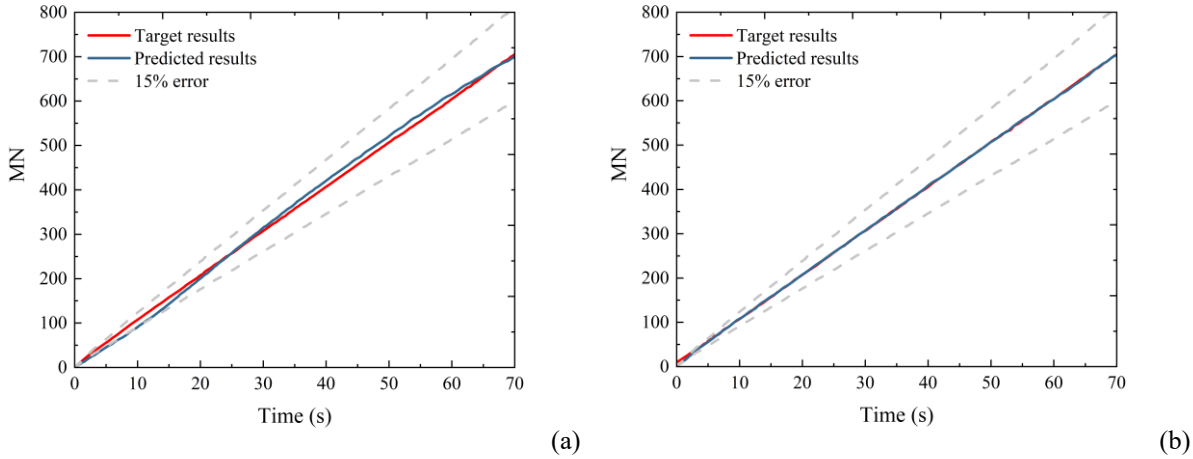

Fig. 6 Comparison of results for the simulation models (a) without PID and (b) with PID

3. Experimental results of the piling operation

This study investigated the platform leg piling behavior in sandy soil, cohesive soil, sand-over-clay, and hard-over-soft soil layers through hydraulic simulation and platform experiments.

3.1 Sandy and cohesive soil layers

Based on the methods and conditions for the piling experiments of jack-up drilling platform legs described in reference [21], the parameters of sandy and cohesive soil layers required for the experiment were configured. The variation curves of soil bearing capacity during the actual piling process in these soil layers were obtained using a hydraulic simulation model, as depicted in Figure 7. The predicted result curve exhibits a high degree of alignment with the form of the target curve [21], accompanied by negligible error, which indicates the system's high control accuracy and stability. Furthermore, the simulation results effectively replicated the piling process of platform legs in single-layer sandy and cohesive soils.

A comparison of the dynamic response characteristics between the hydraulic simulation curve (experimental results) and the target soil curve reveals significant differences in the displacement-pressure relationship during the initial piling stage, as illustrated in Figure 8. To clearly demonstrate the degree of agreement between the predicted results and the reference data, a reference line representing a 15 % error margin was graphed. During the initial pressurization stage, the pressure rise rate of the actual piling test curve lagged behind the target curve by approximately 15 %, potentially attributable to the compressibility of the hydraulic fluid within the system, resulting in insufficient initial energy transfer efficiency. Throughout the mid-stage dynamic regulation phase, the actual pressure curve exhibited high-frequency minor oscillations

(with an amplitude of about ±8 %), contrasting with the smooth upward trend of the target curve. The actual pressure remained consistently lower than the target, with a maximum absolute error (*MAE*) of 13 % and Root Mean Square Error (*RMSE*) of 8.4 % across the full displacement range.

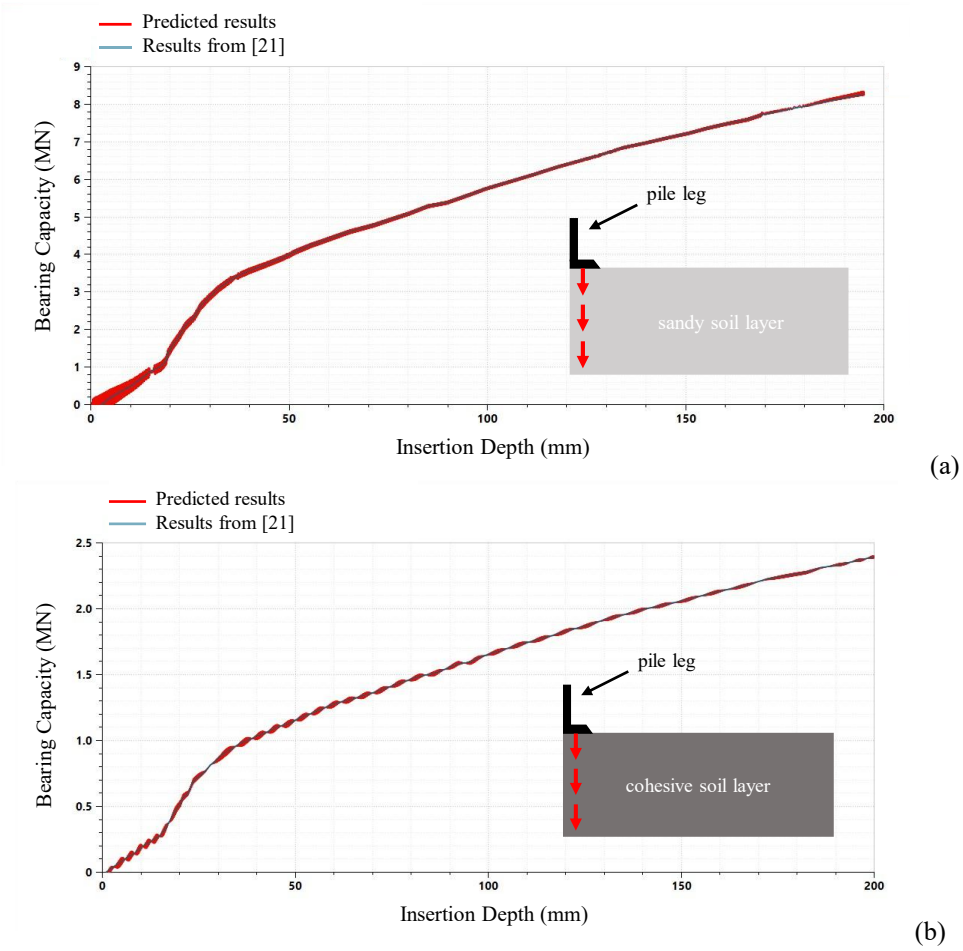

Fig. 7 Predicted results of the hydraulic simulation model for (a) sandy soil layer and (b) cohesive soil layer

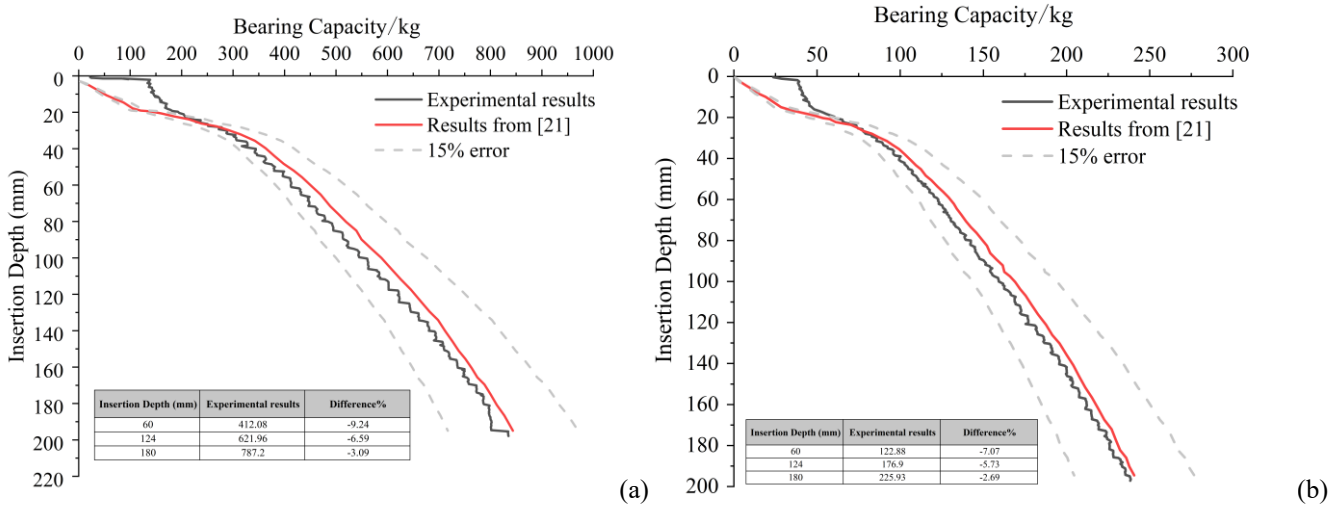

Fig. 8 Experimental results of foundation bearing capacity for (a) sandy soil layer and (b) cohesive soil layer

3.2 Sand-over-clay soil layer

The bearing capacity of the sand-over-clay soil layer was calculated using the Hanna & Meyerhof method and the projected area method. The parameters required for the sand-over-clay soil layer experiment were configured based on reference [22]. The variation curve of soil bearing capacity during the actual piling

process in the sand-over-clay soil layer was obtained via the hydraulic simulation model, as shown in Figure 9. The actual bearing capacity curve during the platform leg penetration process was obtained through hydraulic platform experiments, as shown in Figure 10. The comparison shows that the overall pressure-displacement response trends during the piling process were generally consistent between the two.

In the initial stage, the actual pressure values (experimental results) were slightly higher than the target curve, possibly due to transient overshoot in the hydraulic system response. In the mid-stage (displacement range 1.2-3 m), the two curves were closely aligned, indicating favorable control adaptability of the hydraulic platform for the homogeneous soil segment. In the later stage (displacement > 3 m), the prediction results curve was in satisfactory agreement with the target curve.

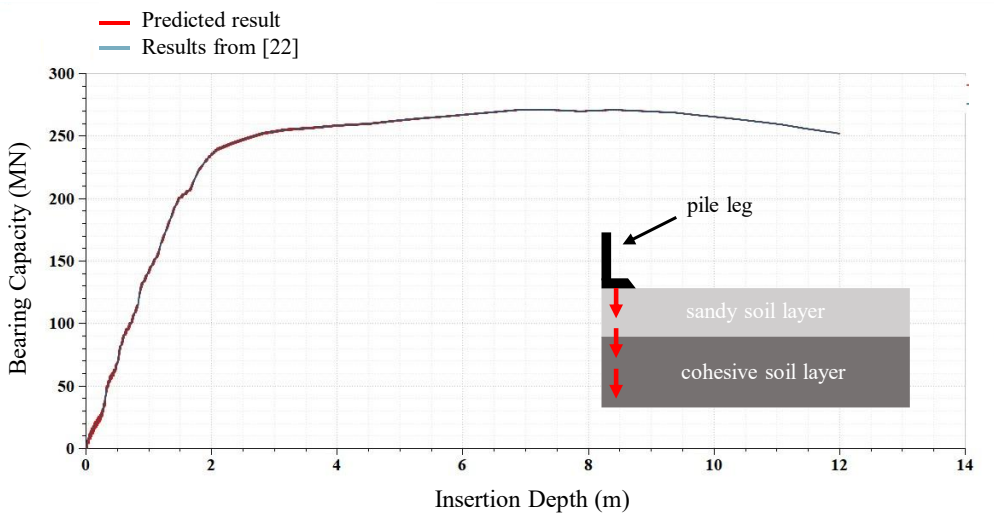

Fig. 9 Predicted results of the hydraulic simulation model during the leg piling process for sand-over-clay soil layer

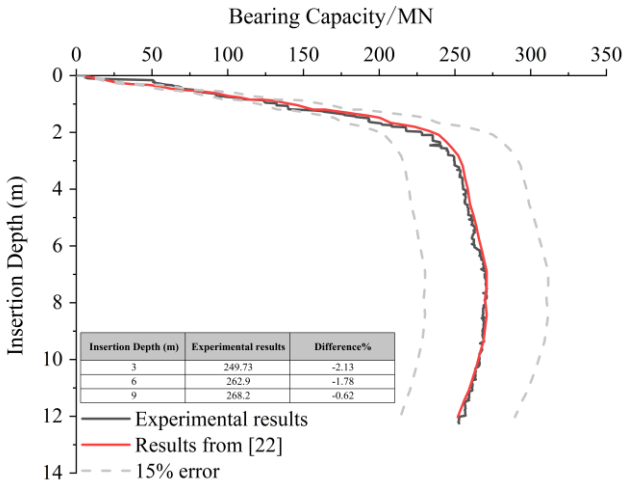

Fig. 10 Experimental results of foundation bearing capacity during the leg piling process for sand-over-clay soil layer

3.3 Hard-over-soft soil layer

Taking a self-elevating drilling platform with a working water depth of 400 feet as an example, Lin et al. [22] analyzed the risk of a pile cap piercing accident that may occur during pre-ballast operations in a certain sea area of the Gulf of Mexico using the Monte Carlo method. The undrained shear strength ratio between the upper and lower soil layers is set to C_{u1}/C_{u2}=1.5, where C_{u1} and C_{u2} represent the undrained shear strengths of the upper hard clay and lower soft clay, respectively. The pile driving process of the pile leg in the hard-over-soft clay layer was simulated using a hydraulic simulation model, and the obtained simulation curve is shown in Figure 11. The prediction results curve is closely aligned with the target curve, with minimal error.

Figure 12 presents a comparison between the platform pile driving test curve and the target soil layer curve. In the initial stage (displacement range 0-4 m), the actual pile driving test curve closely coincided with

the target soil layer. During the mid-stage (displacement range 4-22 m), the actual curve displayed low-frequency periodic fluctuations, with an amplitude of approximately ±8 % of the target value. These fluctuations may be attributed to the step response delay of the hydraulic servo valve and phase lag in the control loop. In the later stage (displacement > 22 m), the pile leg enters the underlying soft soil layer with significantly lower shear strength compared with the overlying stiff soil, leading to a rapid decrease in bearing capacity. The actual pressure values (experimental results) gradually coincided with those of the target soil layer. Overall, the hydraulic platform can effectively simulate the conditions of hard-over-soft soil layer in this scenario. The *RMSE* and *MAE* for this configuration are 6.9 % and 12.1 %, respectively, particularly concentrated near the transition depth.

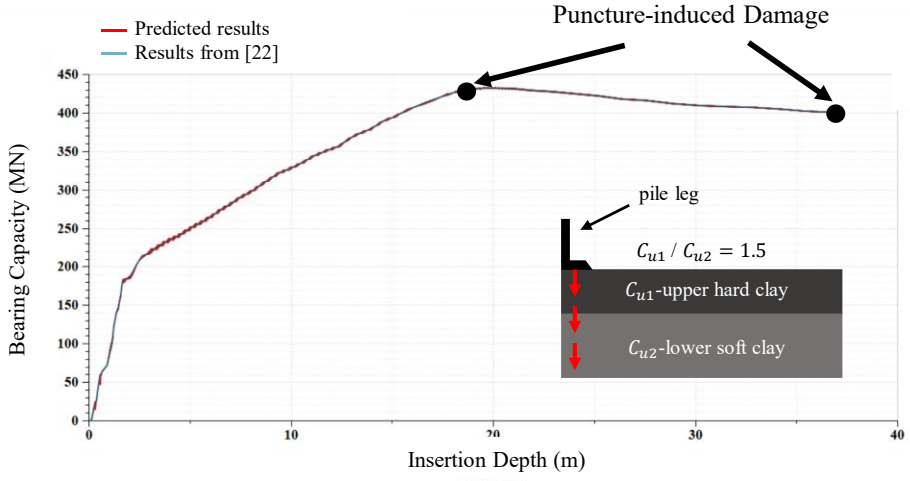

Fig. 11 Hydraulic simulation model prediction results during pile leg driving process for hard-over-soft soil layer

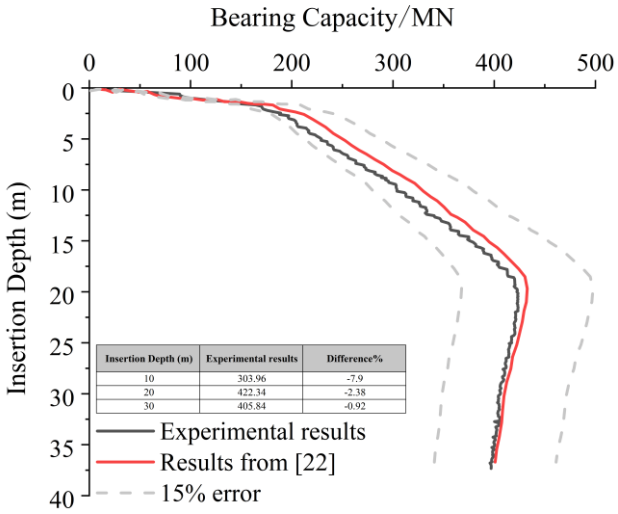

Fig. 12 Foundation bearing capacity test results during pile leg driving process for hard-over-soft soil layer

4. Pile leg penetration test results and analysis

The variation in bearing capacity during the process of pile driving under penetration conditions was investigated through a series of simulation analyses and experimental tests, with soil shear strength, layer thickness, and backfill effects accounted. Prior to soil penetration tests, the PID-controlled servo-hydraulic system was validated using step and sinusoidal reference tracking. The results confirmed that the closed-loop system maintained stable operation, with negligible steady-state error and satisfactory dynamic tracking performance.

4.1 Pile leg penetration in soft-hard-soft layered clay

Building upon centrifuge model tests regarding jack-up drilling platform penetration mechanisms in stratified soils, different soil strengths were consolidated via centrifuge and other methods to prepare soft and hard soil layers, arranged into a soft-hard-soft soil configuration [23]. The penetration process of the platform leg through the soft-hard-soft layered soil was simulated using a hydraulic model, and the simulation results are shown in Figure 13. The predicted results curve closely matched the target curve with minimal error, indicating that the simulation model faithfully reproduced platform leg piling and penetration process within this specific soil stratification. The centrifuge method requires extensive physical preparation, resulting in prolonged preparation periods. In contrast, the hydraulic platform enables rapid switching among different soil layer parameters through simple input of control signals, demonstrating significant advantages in operational efficiency. Furthermore, centrifuge testing is inherently constrained by scale effect and model size. The hydraulic platform can achieve flexible simulation of multiple typical geotechnical conditions, such as sandy soil, clay, hard-soft alternating layers, and soft-hard-soft stratifications, and support repeated testing in continuous loading scenarios.

The actual bearing capacity curve of the platform leg penetrating through the soft-hard-soft layered soil was obtained via hydraulic platform experiments, as shown in Figure 14. The piling test curve and the target soil layer curve were basically consistent in overall trend, demonstrating segmented characteristics corresponding to the soft-hard-soft soil layers. The test curve exhibited a relatively small slope in the initial transition stage from the soft to hard soil layer, warranting sensitivity improvement of the hydraulic simulation platform to changes in soil stiffness. In the intermediate penetration stage, the target soil layer curve displayed a sharp bearing capacity peak within the hard soil segment, whereas the test curve response was smoother in this region, with pressure amplitudes falling below the target value and exhibiting a response lag of approximately 10-15 %. Such discrepancy is attributable to insufficient pressure buildup rate within the hydraulic system, resulting in systemic delay. In the initial operational stage, the control system issues commands corresponding to relatively low hydraulic pressures. Under these conditions, the impact of oil supply delay on the experimental outcomes remains especially pronounced. However, as the hydraulic pressure associated with the control command increases, the impact of this delay diminishes significantly. During the penetration phase from hard to soft soil, the target soil curve exhibited a significant drop in bearing capacity, with characteristics of penetration.

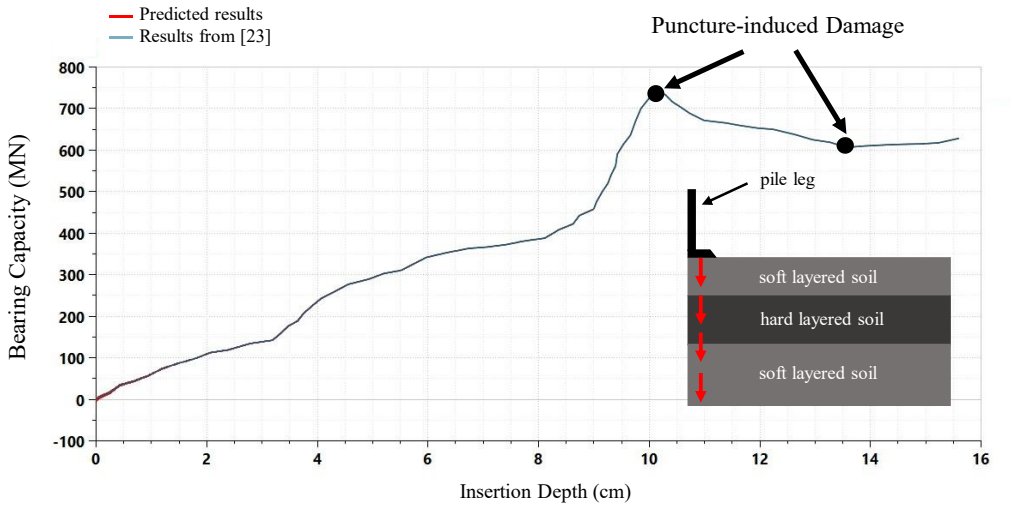

Fig. 13 Predicted results of the hydraulic simulation model for platform leg penetration in soft-hard-soft layered soil

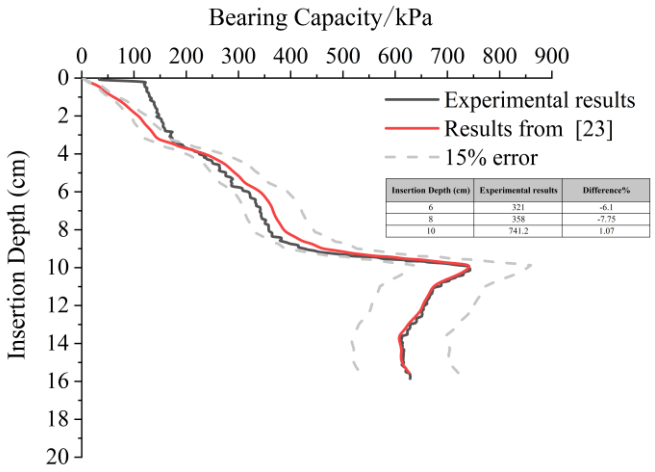

Fig. 14 Experimental results of platform leg penetration in soft-hard-soft layered soil

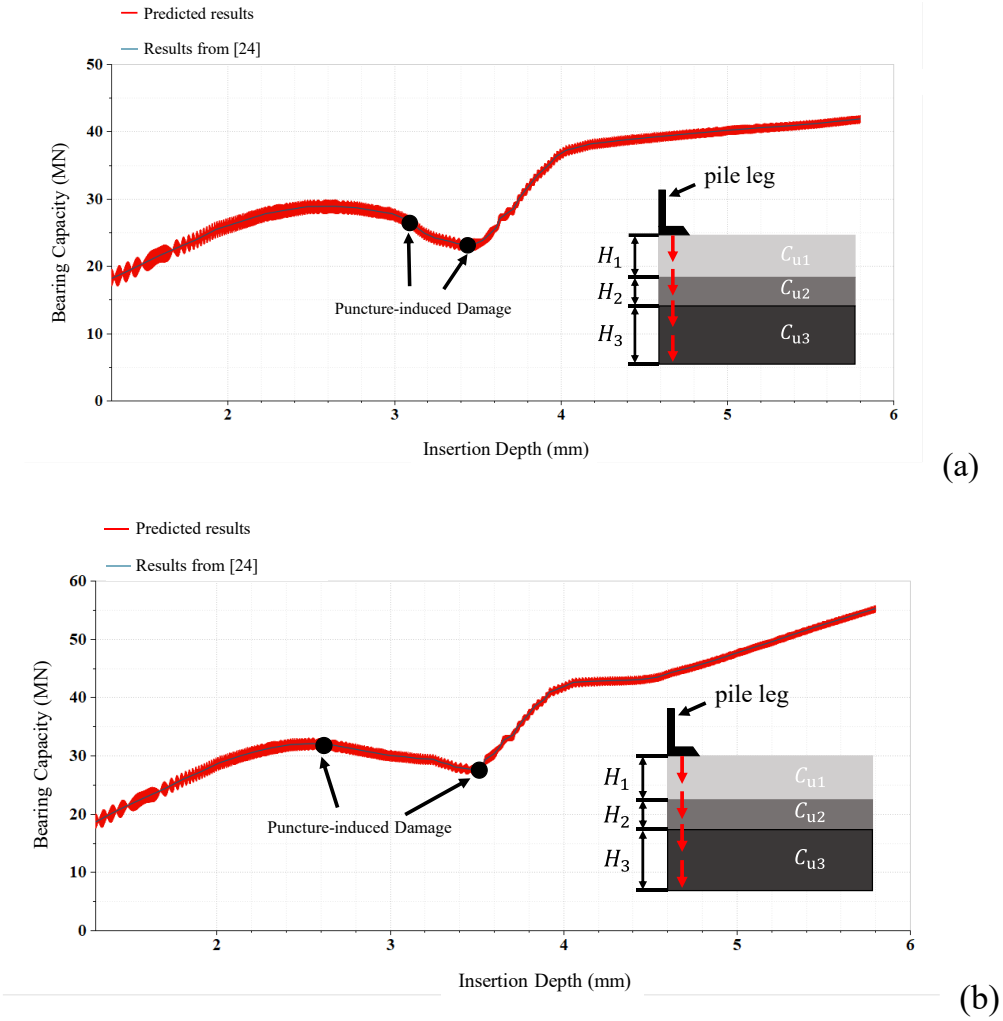

Fig. 15 Predicted results of the hydraulic simulation model for platform leg penetration (a) C_{u2} =150 kPa and (b) C_{u2} =37.5 kPa

4.2 Effect of shear strength of the intermediate hard soil layer

Two conditions of different shear strengths of the platform leg in this soil layer were simulated using the hydraulic simulation model, as shown in Figure 15. The top and bottom layers were soft clay, with a hard clay intermediate layer [24]. The thicknesses of the soft and hard clay layers are denoted as H_1 = 4.5 m and H_2 = 1 m, where H_1 and H_2 represent the thicknesses of the upper hard and lower soft clay layers, respectively. The top and bottom soft clay layers are composed of the same clay type, with an undrained shear strength of C_{u1} =

C_{u3} = 30 kPa. The undrained shear strength of the intermediate hard clay layer is set to be 1.25 times and 5 times that of soft clay, i.e., C_{u2} = 37.5 kPa and 150 kPa, respectively. The actual bearing capacity curve during the process of platform leg penetration was obtained through hydraulic platform experiments, as shown in Figure 16. The general response trends showed consistency, with an *RMSE* of 7.1 % and *MAE* of 11.6 %, confirming that the jack-up hydraulic platform effectively simulated the penetration behavior under varying C_{u2} conditions. Initial stage testing revealed a slight response lag compared with the target soil curve, potentially attributable to hydraulic system delay. Near the soil punch-through point during intermediate stages, the test curve followed the target trend but displayed a slight decrease in peak pressure and somewhat slower displacement rates, possibly derived from the full replication of the target conditions hindered by hydraulic system output saturation. In the late-stage bearing capacity peak region, the test curve pressure was slightly lower than that of the target soil curve, with the error possibly due to limitations in the force control accuracy of the hydraulic system.

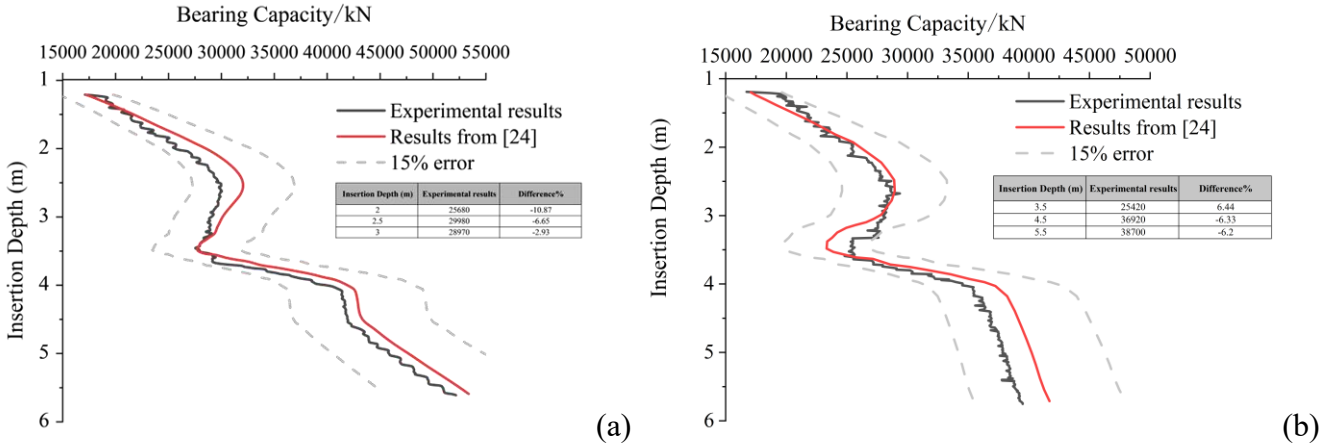

Fig. 16 Experimental results of platform leg penetration (a) C_{u2} = 150 kPa; (b) C_{u2}= 37.5 kPa

4.3 Considering the effect of soil backfill

Zhou et al. [25] investigated the bearing capacity of geological soil layers at a jack-up offshore platform site in the South China Sea, considering two scenarios: unbackfilled and fully backfilled. On this basis, appropriate parameter configurations were established for the layered foundation. The simulation results obtained are shown in Figure 17. The predicted result curve closely matches the target curve, with minimal error.

The experimental bearing capacity curve incorporating backfill effects obtained through hydraulic platform testing is shown in Figure 18. Both exhibit segmented characteristics of the layered soil, but systematic deviations have emerged in critical regions. In the initial piling stage, the trends of both curves were relatively consistent; however, the experimental curve showed slightly higher stiffness than the target curve in the initial loading segment. Near the penetration point (corresponding to the transition zone of soil layer structure), the experimental curve exhibited a lagged pressure response, and the displacement growth rate showed brief fluctuations during the penetration process, failing to fully replicate the smooth transition of the target soil curve. This error is mainly derived from differences in the data phase due to sensor sampling frequency and control system delay, resulting in reduced timing match during the penetration process. In the later stage, the overall trends of both were basically consistent.

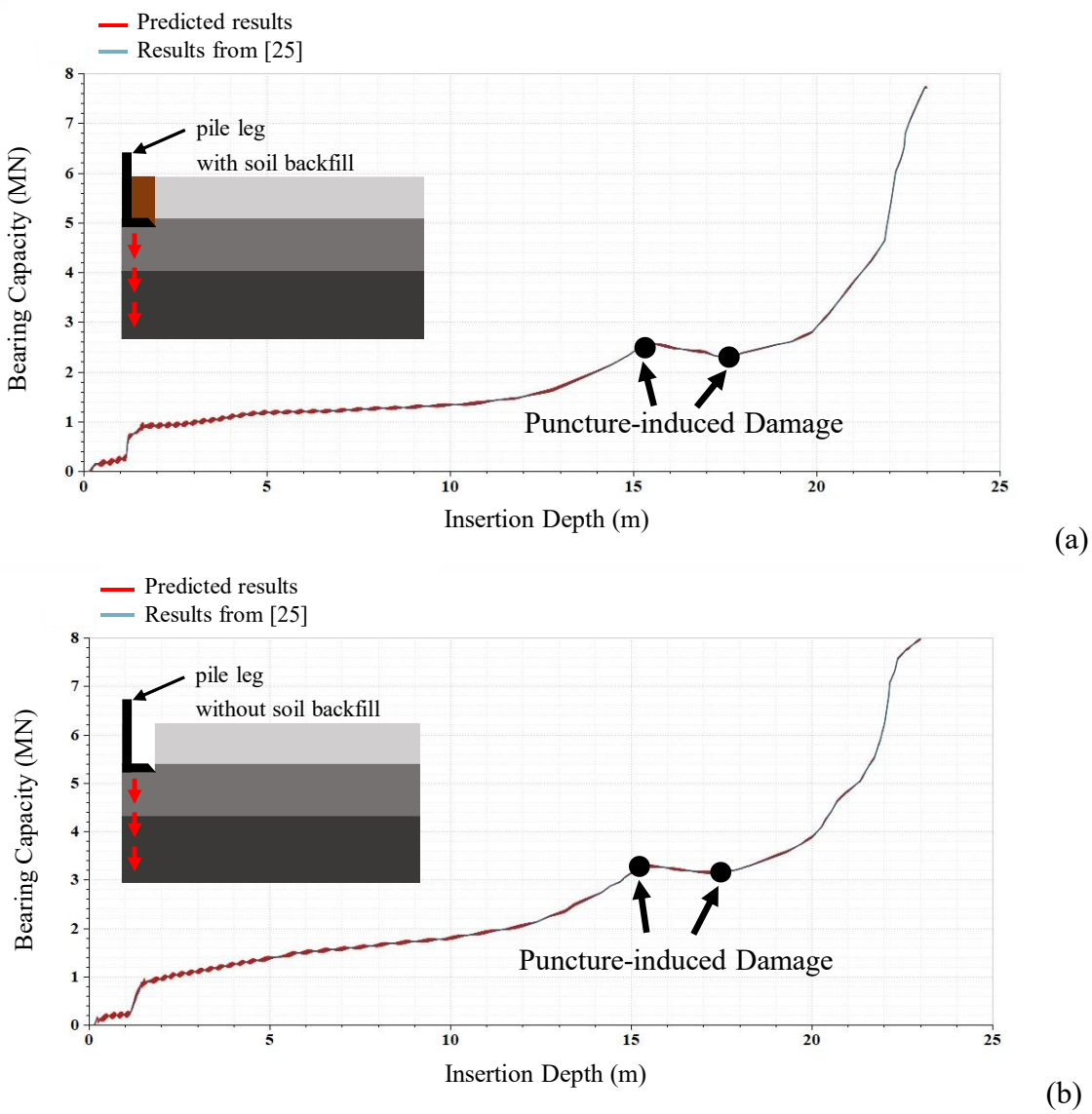

Fig. 17 Predicted results of the hydraulic simulation model for platform leg penetration considering (a) fully backfilled and (b) unbackfilled

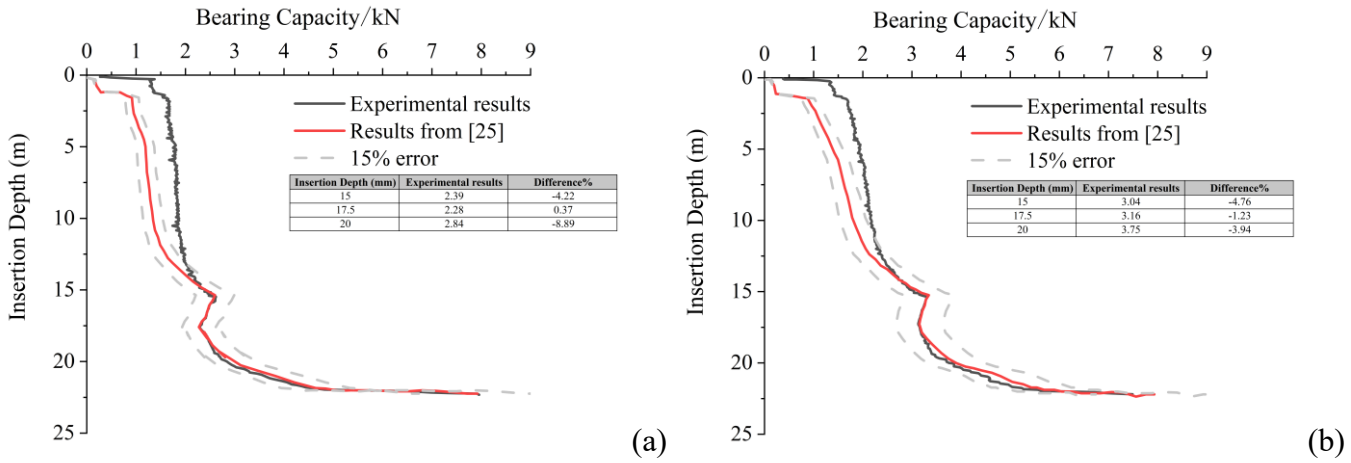

Fig. 18 Experimental results of platform leg penetration considering (a) complete backfill and (b) no backfill

4.4 Effect of hard soil layer thickness

Soft clay was selected as the soft soil layer, and reinforced sand was used as the hard soil layer to configure a hard-over-soft soil profile, as shown in Figure 19(a). The soft clay layer was set to a thickness of

approximately 10 cm, and two different thicknesses of hard layer, namely 10 and 15 cm, have been selected [21]. The penetration process of the platform leg through the soil layers was simulated using the hydraulic model, and the soil bearing capacity curves obtained are shown in Figure 19. The predicted results curve closely matched the target curve, with minimal error.

The actual bearing capacity curve of the platform leg penetration through the egg-shell stratigraphy was obtained via hydraulic platform testing, as shown in Figure 20. In the upper hard soil layer stage, the pressure response trends of both curves were highly consistent, indicating the ability of the hydraulic system to accurately simulate the mechanical properties of the hard soil. In the transition zone from the intermediate soft clay to the bottom sand layer (near the penetration point), the target soil curve displayed a remarkable decrease in bearing capacity, while the experimental response showed a slight delay with moderately reduced peak values. This deviation was probably due to hydraulic system dynamic response lag, preventing timely output adjustment to simulate rapid instability of soft soil. During the process of bottom sand layer penetration, the target curve showed pressure recovery and stability due to high sand frictional resistance. Such phenomenon is accurately reproduced by the experimental curve.

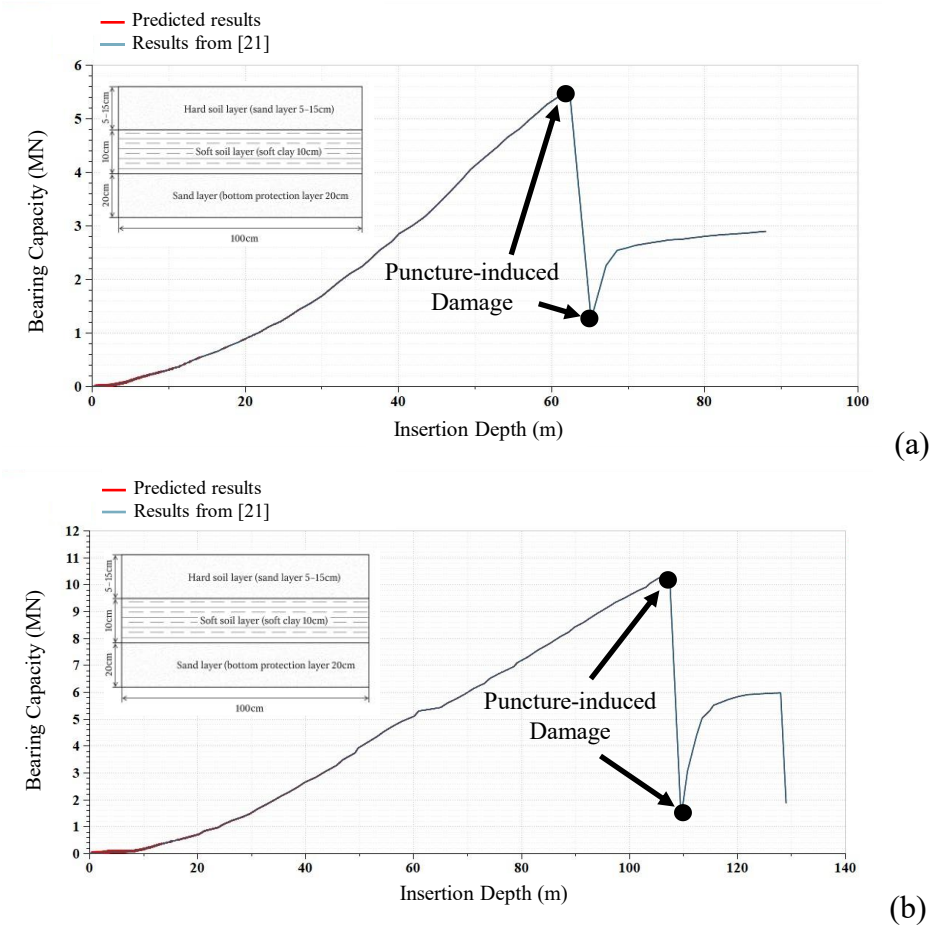

Fig. 19 Predicted results of the hydraulic simulation model for platform leg penetration for hard soil layer (a) 10 cm and (b) 15 cm

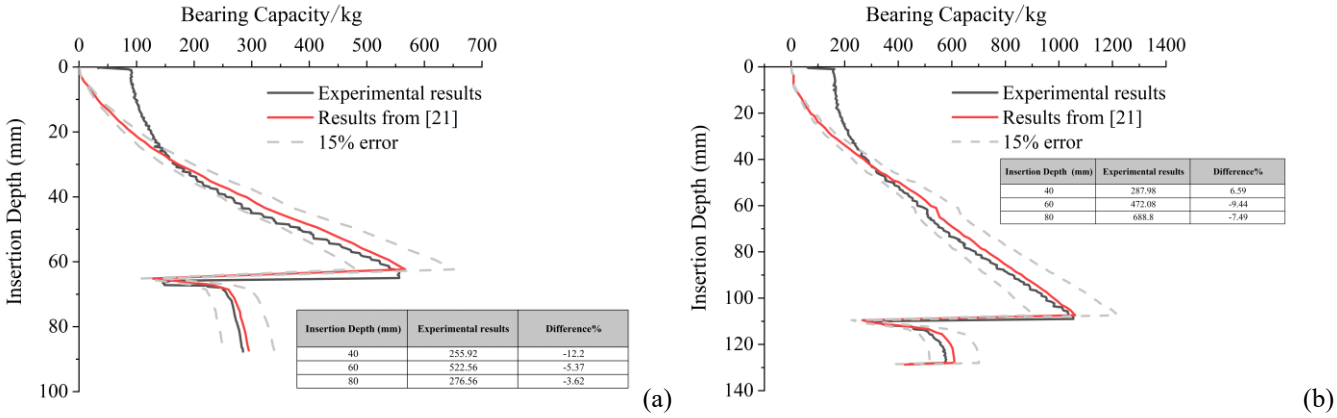

Fig. 20 Experimental results of platform leg penetration for hard soil layer (a)10 cm and (b) 15 cm

Table 1 The difference of experimental results

No.	Soil layer type	Insertion Depth	Experimental results	Difference %
1	sandy soil layer	60	412.08	-9.24
		124	621.96	-6.59
		180	787.2	-3.09
2	cohesive soil layer	60	122.88	-7.07
		124	176.9	-5.73
		180	225.93	-2.69
3	sand-over-clay soil layer	3	249.73	-2.13
		6	262.9	-1.78
		9	268.2	-0.62
4	hard-over-soft soil layer	10	303.96	-7.9
		20	422.34	-2.38
		30	405.84	-0.92
5	soft-hard-soft layered soil	6	321	-6.1
		8	358	-7.75
		10	741.2	1.07
6	intermediate hard soil layer: C_{u2} = 150 kPa	2	25680	-10.87
		2.5	29980	-6.65
		3	28970	-2.93
7	intermediate hard soil layer: C_{u2}= 37.5 kPa	3.5	25420	6.44
		4.5	36920	-6.33
		5.5	38700	-6.2
8	complete backfill	15	2.39	-4.22
		17.5	2.28	0.37
		20	2.84	-8.89
9	no backfill	15	3.04	-4.76
		17.5	3.16	-1.23
		20	3.75	-3.94
10	hard soil layer thickness :10 cm	40	255.92	-12.2
		60	522.56	-5.37
		80	276.56	-3.62
11	hard soil layer thickness :15 cm	40	287.98	6.59
		60	472.08	-9.44
		80	688.8	-7.49

4.5 Quantitative analysis of test difference

A quantitative error analysis was conducted by comparing the experimental values of bearing capacity at three different insertion depths under each working condition with the values reported in the literature, as presented in Table 1. In the majority of cases (e.g., No. 1, 2, 3, 4, 6, and 10), a consistent tendency has been discerned: as the insertion depth increases, the absolute disparity between the experimental and literature values diminishes, signifying a closer alignment with theoretical or reference values of the measurements at greater depths. However, this tendency was not uniformly manifested in specific soil configurations. In the soft-hard-soft layered soil (No. 5), negative differences were registered at both the shallowest and deepest depths, whereas a positive difference of 1.07 % occurred solely at the intermediate depth (100 cm), presumably due to the probe being located within the hard layer. Overall, the prediction error of the model developed in this study lies predominantly within the range of -13 to +7 %, rendering it suitable for supporting exploratory investigations into underlying patterns - thereby serving as a computationally efficient complement to physical marine foundation experiments.

5. Conclusion

This study introduced a precise control system utilizing pressure proportional valves to experimentally simulate the piling and penetration behavior of jack-up offshore platforms on layered seabed foundations. By integrating the development of a hydraulic simulation system, servo control simulation, and piling experiments, this research overcame the constraints associated with conventional soil layer simulation techniques. The main findings are as follows:

(1) A high-precision dynamic simulation of seabed foundation settlement under varying depth gradients and soil stiffness has been successfully achieved by integrating foundation settlement simulation mechanisms integrated at the leg bases combined with dynamically regulated proportional pressure valves.

(2) The implementation of a PID control algorithm within the proportional valve system has realized dynamic hydraulic compensation. Incorporating the damping parameters of typical seabed soils-sandy, cohesive, and layered composites-multi-condition simulations effectively reproduced the nonlinear soil damping effects during the piling process.

(3) The hydraulic system exhibited high accuracy in hard soil simulation, but response delays and peak errors during the process of soft soil penetration, with an overall error of less than 15%. Subsequent research is beneficial by using adaptive or gain-scheduled PID control, incorporating temperature-dependent viscosity, integrating real-time soil parameter detection to enable adaptive control logic, and conducting sea trials to validate simulation results.

ACKNOWLEDGEMENTS

The current work is supported by the Natural Science Foundation of Zhejiang Province (LTGG23E090003) and the Zhejiang Province “Pointer” and “Leader Goose” R&D Program of Zhejiang (2023C01089).

NOMENCLATURE

C_u	Undrained shear strength
C_{u1}	C_u of the upper soil
C_{u2}	C_u of the second soil
C_{u3}	C_u of the lower soil
C_{u1}/C_{u2}	Shear strength ratio
D_C	Actual displacement
D_R	displacement regulated by hydraulic control
D_{TC}	feedback displacement
D_{TR}	displacement at the insertion point

F_{TC}	actual output bearing capacity
F_{TR}	actual bearing capacity
H	thicknesses of clay layers
H_1	H of the upper soil clay layers
H_2	H of the second soil clay layers
H_3	H of the lower soil clay layers
k	Sampling index
k_p	Proportional gain
PID	Proportional-Integral-Derivative
T	Sampling interval
U_{TC}	Feedback signal voltage
U_R	Input signal voltage
β	Conversion coefficient

APPENDIX A - Apparatus Details

The piling process of the pile leg was simulated through the hydraulic system model, and the technical specifications that each piece of equipment must meet during the normal operation of the hydraulic system were determined. Furthermore, considering an appropriate safety margin, the parameter values of the main hydraulic system components are presented in Table A1. The specifications and parameters of all hydraulic components in the model, including the main pump station, proportional valve group, hydraulic cylinders, and accumulator, were identical to those of the actual equipment.

Table A1 Parameter settings of the hydraulic system model

Component	Parameters	Component	Parameters
Electric motor	1320 rev/min	Overflow valve	1330 rev/min;300 cc/min
Hydraulic cylinder diameter	230 mm	Hydraulic cylinder piston rod diameter	155 mm
Hydraulic motor	1310 rev/min	Signal source of the solenoid valve	0-10 s: 20 null;10-15 s: 0 null; 15-25 s: -20 null
Three-position four-way solenoid valve	Maximum flow rate 450 l/min; damping ratio 1.7		

REFERENCES

[1] Garašić, I., Kralj, S., Kožuh, Z., Pacak, M., 2010. Analysis of underwater repair technology on the jack-up platform spud can. *Brodogradnja*, 61(2), 153-160.

[2] Wang, B., Jiao, Y., Qiao, D., Gao, S., Li, T., Ou, J., 2023. Modified p-y curves for monopile foundation with different length-to-diameter ratio. *Brodogradnja*, 74(2), 149-167. https://doi.org/10.21278/brod74208

[3] Vatsvåg, P. V., 2014. Evaluation of jack-up units in deeper water in the North Sea. *Master's thesis*. University of Stavanger, Norway.

[4] Martin, C., 1994. Physical and numerical modelling of offshore foundations under combined loads. *Doctoral dissertation*, Oxford University, UK.

[5] Hossain, M. S., Randolph, M. F., 2009. Effect of strain rate and strain softening on the penetration resistance of spudcan foundations on clay. *International Journal of Geomechanics*, 9(3), 122-132. https://doi.org/10.1061/(ASCE)1532-3641(2009)9:3(122)

[6] Korzani, M. G., Aghakouchak, A. A., 2015. Soil-structure interaction analysis of jack-up platforms subjected to monochrome and irregular waves. *China Ocean Engineering*, 29, 65-80. https://doi.org/10.1007/s13344-015-0005-3

[7] Fan, L. D., Purwana, O. A., Yuan, Y., Duan, M. L., Gao, J., 2023. Discrete element method for simulations of the jack-up foundation penetration. *Ocean Engineering*, 273, 113884. https://doi.org/10.1016/j.oceaneng.2023.113884

[8] Kong, V., Cassidy, M. J., Gaudin, C., 2015. Failure mechanisms of a spudcan penetrating next to an existing footprint. *Theoretical and Applied Mechanics Letters*, 5(2): 64-68. https://doi.org/10.1016/j.taml.2014.12.001

[9] Xu, J., Zhou, Y., Xue, Q. L., Liao, Q. H., Cui, G. J., Xie, T., Li, H. Y., 2023. Research on risk analysis method of jack-up drilling platform pile leg puncture. *Chemistry and Technology of Fuels and Oils*, 59(1), 1-8. https://doi.org/10.1007/s10553-023-01519-3

[10] Michalowski, R. L., Shi, L., 1995. Bearing capacity of footings over two-layer foundation soils. *Journal of Geotechnical Engineering*, 121(5), 421-428. https://doi.org/10.1061/(ASCE)0733-9410(1995)121:5(421)

[11] Hossain, M. S., Randolph, M.F., 2010. Deep-penetrating spudcan foundations on layered clays: centrifuge tests. *Géotechnique*, 60(3), 157-170. https://doi.org/10.1680/geot.8.P.039

[12] Hossain, M. S., Randolph, M. F., 2010. Deep-penetrating spudcan foundations on layered clays: numerical analysis. *Géotechnique*, 60(3), 171-184. https://doi.org/10.1680/geot.8.P.040

[13] Zhang, Q. Y., Liu, Z. J., 2018. Influence of the spudcan angle on the ultimate bearing capacity of jack-up platform. *China Ocean Engineering*, 32(4), 476-481. https://doi.org/10.1007/s13344-018-0050-9

[14] Yi, M. S., Park, J. S., 2025. Nonlinear analysis and weight optimization of living quarters for offshore jack-up rigs: A sustainable engineering approach. *Applied Ocean Research*, 158, 104515. https://doi.org/10.1016/j.apor.2025.104515

[15] Zhang, Q., Zhu, W., Ye, G., Tian Y. H., Yan Y. Z., 2023. Centrifuge tests and numerical simulations on vertical bearing capacity of mat foundation on marine clay seabed. *Applied Ocean Research*, 135, 103534. https://doi.org/10.1016/j.apor.2023.103534

[16] Zhao, J., Jang, B. S., Duan, M., Liang, C., 2019. A finite element approach for predicting the full resistance profile of a spudcan deeply penetrating in dense sand overlying clay. *Applied Ocean Research*, 87, 155-164. https://doi.org/10.1016/j.apor.2019.03.026

[17] Kellezi, L., Sundararajan, S. S., Lundvig, K. H., 2019. Seabed remediation avoiding critical spudcan-boulder interaction during jack-up vessel installations in offshore wind. *The 17th International Conference*: *The Jack-Up Platform Design, Construction & Operation*, September 12-13, London, UK.

[18] Houlsby, G. T., 2016. Interactions in offshore foundation design. *Géotechnique*, 66(5), 366-384. https://doi.org/10.1680/jgeot.15.RL.001

[19] Osborne, J. J., Houlsby, G. T., Teh, K. L., Bienen, B., Cassidy, M. J., Randolph, M. F., Leung, C. F., 2009. Improved guidelines for the prediction of geotechnical performance of spudcan foundations during installation and removal of jack-up units. *The 41st Offshore Technology Conference*, May 4-7, Houston, Texas, USA. https://doi.org/10.4043/20291-MS

[20] Ardavanis, K., Nabergoj, R., Mauro, F., 2022. DP challenges in ANA platform jacket installation. *Brodogradnja*, 73(4), 1-11. https://doi.org/10.21278/brod73401

[21] Yin, Q., Yang, J., Xu, G., Xie, R., Tyagi, M., Li, L., Zhou, X., 2020. Field experimental investigation of punch-through for different operational conditions during the jack-up rig spudcan penetration in sand overlying clay. *Journal of Petroleum Science and Engineering*, 195, 107788. https://doi.org/10.1016/j.petrol.2020.107823

[22] Lin, Y., Hu A. K., Jiang, W., Wang, Y. T., 2016. Risk analysis of punch through for jack-up drilling unit in layered soil. *Journal of Harbin Engineering University*, 37(6): 754-761.

[23] Li, S., Wang, Y. C., Wu, X. Z., Liang, J. H., Zhou, Y. R., 2015. Centrifugal model tests on mechanism of spudcan penetration of jack-up drilling platform in egg-shell layered soil. *Chinese Journal of Geotechnical Engineering*, 37(3), 479-486. https://doi.org/10.11779/CJGE201503011

[24] Xu, G., Liu, S., Tong, G., Yin, Q., Hu, N., 2019. Research on spud leg's driving depth prediction and punch-through potential analysis of jack-up drilling platform. *The 29th International Ocean and Polar Engineering Conference*. June 16-21, Honolulu, Hawaii, USA.

[25] Zhou, H., Luo, P. P., Zhou, F., 2015. Effect of changing geological parameters in South China Sea on the bearing capacity of foundations and puncture assessment. *Ship Engineering*, 12, 98-102.